Int. J. Multiphase Flow Vol. 15, No. 1, pp. 23–34, 1989
Printed in Great Britain.

0301-9322/89 $3.00 + 0.00

THE RELATIONSHIP BETWEEN INTERFACIAL SHEAR AND FLOW PATTERNS IN VERTICAL FLOW

A. YING† and J. WEISMAN
Department of Chemical and Nuclear Engineering, University of Cincinnati, Cincinnati, OH 45221, U.S.A.

(*Received* 31 *March* 1988; *in revised form* 11 *September* 1988)

Abstract—The relationship between interfacial shear and the flow patterns observed in the vertical upflow and downflow of vapor–liquid mixtures has been explored. It was found that the flow pattern transitions in adiabatic flow could be related to the interfacial shear. New observations of the two-phase flow behavior of refrigerant 113 in heated lines indicated that the void fraction vs quality curves and the location of some flow pattern transitions differ under adiabatic and diabatic conditions. The shifts seen in the flow pattern transitions are consistent with the changed interfacial shear derived from the revised void fraction vs quality curves.

Key Words: two-phase flow, interfacial shear, flow patterns

1. PREVIOUS EVALUATIONS OF INTERFACIAL SHEAR

1.1. Basic approach

The more sophisticated computer programs used for analysis of the transient behavior of systems containing vapor–liquid mixtures allow for differing phase velocities and the lack of thermodynamic equilibrium. These programs must therefore estimate the rates of interphase mass, momentum and energy transfer. A convenient way of dealing with the rate of momentum transfer is through the dynamic model of McFadden *et al.* (1981). This model, which is incorporated in the RETRAN computer code, is based upon a differential equation (dynamic slip equation) describing the change in the relative velocity of the phases. It is derived by writing the momentum equations for the liquid and vapor, subtracting and then solving for the time derivative of the differential velocity.

The use of the dynamic equation of McFadden *et al.* (1981) requires values for the product of interfacial drag and the interfacial area per unit volume, $C_D A_{FG}$. Crawford *et al.* (1985) showed that values of $C_D A_{FG}$ may be computed from a knowledge of the presssure drop per unit length and the relationship between quality and void fraction in the steady state. Crawford *et al.* (1985) also presented a set of curves providing values for $C_D A_{FG}$ for the refrigerant 113 system in downward flow.

Subsequently, Ying & Weisman (1988) observed that the expressions of McFadden *et al.* (1981) and Crawford *et al.* (1985) need to be modified at high mass fluxes. At very high mass fluxes, a two-phase mixture tends to behave like a homogeneous fluid and the interfacial shear approaches zero. To allow for this behavior, an additional term must be introduced. This term may be considered as representing the turbulent, or Reynolds, stresses acting on the vapor–liquid interface, even when there is not difference between the mean velocities of the phases. Ying & Weisman (1988) therefore obtained $C_D A_{FG}$ for adiabatic flow from the following:

$$C_D A_{FG}\left[\frac{\bar{\rho} V_{FG}|V_{FG}|}{8\rho_G(1-\epsilon)}\right] = -\left(\frac{1}{\rho_L}-\frac{1}{\rho_G}\right)\frac{dP}{dz} - \frac{f_{WL} V_L^2}{2D(1-\epsilon)} - \frac{C(\epsilon)[U_{\tau,2\phi}^2 \bar{\rho}]}{2D}, \quad [1]$$

with

$$U_{\tau,2\phi} = \frac{G}{2\bar{\rho}}\left(\frac{0.184}{Re_m^{0.2}}\right)^{1/2}, \quad [2]$$

†Present address: Fusion Engineering Program, UCLA, Los Angeles, CA 90024, U.S.A.

where

A_{FG} = interfacial (gas–liquid) surface area per unit volume (length^{-1}),
A_{WG}, A_{WL} = surface area per unit volume of gas and liquid, respectively, in contact with the wall (length^{-1}),
C_D = interfacial (liquid–gas) drag coefficient,
D = tube diameter (length),
f_{WL} = friction factor between the liquid and the wall,
G = total mass flux (mass/area time),
P = pressure (force/area),

$$\mathrm{Re}_m = \frac{DG}{[\alpha\mu_G + (1-\alpha)\mu_L]},$$

$$U_{\tau,2\phi} = \text{two-phase functional velocity} = \left(\frac{2\tau_w}{\rho_m}\right)^{0.5},$$

V_G, V_L = mean velocities of gas liquid, respectively (length/time),
$V_{FG} = V_G - V_L$,
z = axial distance (length),
ϵ = void (vapor) fraction,
τ_W = wall shear stress,
$\rho_G, \rho_L, \bar{\rho}$ = gas, liquid and average densities, respectively (mass/length^3)

and

μ_G, μ_L = gas and liquid viscosities, respectively.

The parameter $C(\epsilon)$ is a function of the void fraction, ϵ, and its numerical value for a given ϵ is determined at the onset of dispersed flow where $V_{FG} = 0$. We then have

$$\frac{C(\epsilon)[U_{\tau,2\phi}^2\bar{\rho}]}{2D} = -\left(\frac{1}{\rho_L} - \frac{1}{\rho_G}\right)\frac{dP}{dz} - \frac{f_{WL}V_L^2}{2D(1-\epsilon)}. \quad [3]$$

For low and moderate void fractions, the onset of dispersed flow occurs at a constant mass flux. For refrigerant 113 in a 2.5 cm dia tube, this occurs at a mass flux of about 1.5 kg/m^2 h. This mass flux was therefore used to determine $U_{t,2\phi}$ in [3]. The value of dP/dz in [3] was computed assuming homogeneous flow.

Ying & Weisman (1988) used their own and literature data to calculate curves showing the variation of $(C_D A_{FG})$ with G and ϵ, void fraction, for both upflow and downflow of refrigerant 113 and steam–water mixtures. The curves they obtained for refrigerant 113 at 2 b in a 2.5 cm tube are shown in figures 1 and 2. The curves have been made dimensionless by multiplying $C_D A_{FG}$ by the tube diameter, D.

It should be noted that in the computation of $C_D A_{FG}$ for downward flow, V_{FG} was always taken as having a negative value (mean liquid velocity exceeds mean gas velocity). This means that the product $V_{FG}|V_{FG}|$ is taken as negative for downflow and this leads to positive values for $C_D A_{FG}$, except at very high void fractions. The negative value of $C_D A_{FG}$ obtained for annular flow at high voids implies that V_{FG} is actually positive in this region.

1.2. Interfacial shear predictions

Phenomenologically based models for interfacial drag in upward flow have been proposed for use in the TRAC computer program by Hughes *et al.* (1976) and Solbrig *et al.* (1975). Poor agreement is obtained between these predictions and the experimentally derived values of Ying & Weisman (1988). Improved models were more recently proposed by Ishii & Mishima (1980). These later models generally show the same trends as exhibited by the experimentally derived curves of Ying & Weisman (1988) but are not in good agreement with the numerical values.

In view of the foregoing, Ying & Weisman (1988) developed a revised predictive procedure for estimating the values of $C_D A_{FG}$. In their flow-regime-dependent model, the formation of large size bubbles or plugs is assumed to begin when the ratio of (average distance between bubbles)/(bubble

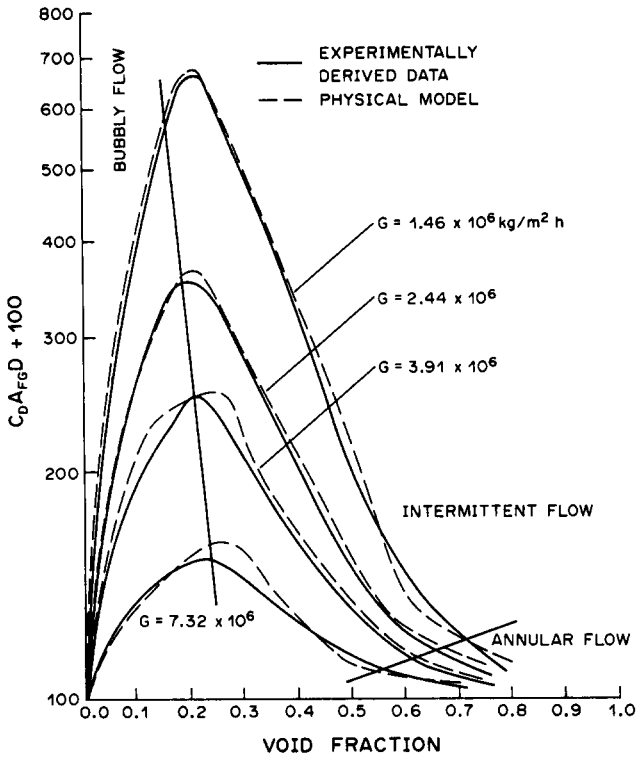

Figure 1. $C_D A_{FG}$ for adiabatic upflow of refrigerant 113 at 2 b.

diameter) falls below a critical value. In calculations at higher void fractions, the interfacial shear has a component from the large size bubbles or gas plugs and an assemblage of small size bubbles. In annular flow, the interfacial shear is the sum of the shear between the gas and the liquid film plus the shear between droplets and gas. In downward flow, the procedure for estimating interfacial shear in the annular region is applied to both the annular and falling film region. At the conditions for a falling film, the model predicts essentially zero entrainment and hence the shear is soley due to the liquid film. The boundary between intermittent and annular or falling film flow is determined by the intersection of the interfacial shear models.

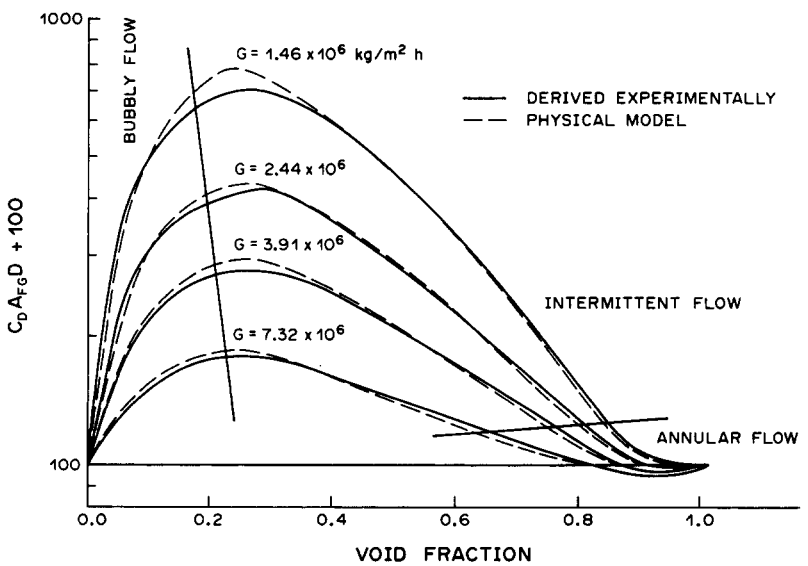

Figure 2. $C_D A_{FG}$ for adiabatic downflow of refrigerant 113 at 2 b.

The Ying & Weisman (1988) model assumes that, when bubbles or droplets get below a critical diameter, they are carried along at the stream velocity and exert no drag. The dispersed flow boundary therefore corresponds to the locus of points at which a zero drag is first computed.

In addition to the experimentally derived curves of $C_D A_{FG}$, figures 1 and 2 show the predictions obtained from the interfacial shear models of Ying & Weisman (1988). It may be seen that the models provide a reasonably good fit of the experimentally derived data.

2. PRESENT STUDY

2.1. Objectives of the study

The basic objective of the study was to explore the relationship between interfacial shear and flow patterns. In the first portion of the study, the previous evaluations of interfacial shear under adiabatic conditions were used to explore this relationship.

In the second portion of the study, a series of experiments were conducted to determine the interfacial shear and flow pattern transitions with heating (diabatic flow). The observed changes in the flow pattern transitions are then explained based upon the changes in interfacial shear.

2.2. Experimental program

The experimental tests were conducted by installing a special heated test section in the University of Cincinnati's boiling refrigerant loop. This facility is capable of circulating up to 110 l/min of refrigerant 113 at moderate pressures. Electric immersion heaters preheat the refrigerant to the temperature or quality desired at the test section inlet. A condenser located at the test section outlet condenses any vapor produced so that the pump sees only liquid. Further details on the loop design may be found in Weisman *et al.* (1988).

A cross-sectional view of the vertical heated test section used is shown in figure 3. The heart of the test section is a 1.83 m (6 ft) long glass tube having an i.d. of 2.54 cm. Heat is supplied by direct a.c. current heating of two curved stainless steel strips placed against opposite sides of the tube. The strips are electrically connected at the bottom so that an external electrical connection need only be made through the cross placed at the upper end of the test section. Piping between the test section and the loop was arranged so that flow could be upward or downward through the test section.

The two 90° circular segments of BWG 20 tubing, which form the heating strips, covered only half the wall area. This allowed clear visual and photographic observation of the behavior along the test section. The clear path provided also allowed void fraction measurements to be made using a γ-densitometer. The γ-densitometer used ^{137}Cs, which emits a 0.66 MeV γ-ray, as the radiation source. A scintillation detector with a linear rate meter was used for measurement of the intensity of the transmitted radiation. A trolley on the front and back of the test section allowed the γ-source and detector to be located at any desired axial location. A micron metal shield around the detector eliminated magnetic field interference from the current-carrying strips. The shielded detector was calibrated against density measurements in a separate adiabatic line.

In addition to flow pattern observations, experimental measurements were made of flow, system pressure and heat input. Flow measurements were obtained by measurement of the pressure drop across a set of standard orifices while system pressure was obtained from an accurate Bourdon gauge. The heat input to the test section was obtained from measurement of the electrical power after a correction for convective losses.

Tests were conducted at a pressure of 2 b. The total flow rate was fixed and then the heat input to the system was increased until a flow pattern transition was seen at some point along the test section. The axial location and void fraction at the transition was observed. For the transition to bubbly flow, subcooled liquid entered the test section. However, in order to observe the transition to annular flow it was necessary to introduce a two-phase mixture at the inlet.

Measurement of the variation of void fraction vs distance along the heated test section were also made under various conditions. The observed void fraction vs distance curves were compared with computations based on the heat input and the relationship between void fraction and quality determined under adiabatic conditions.

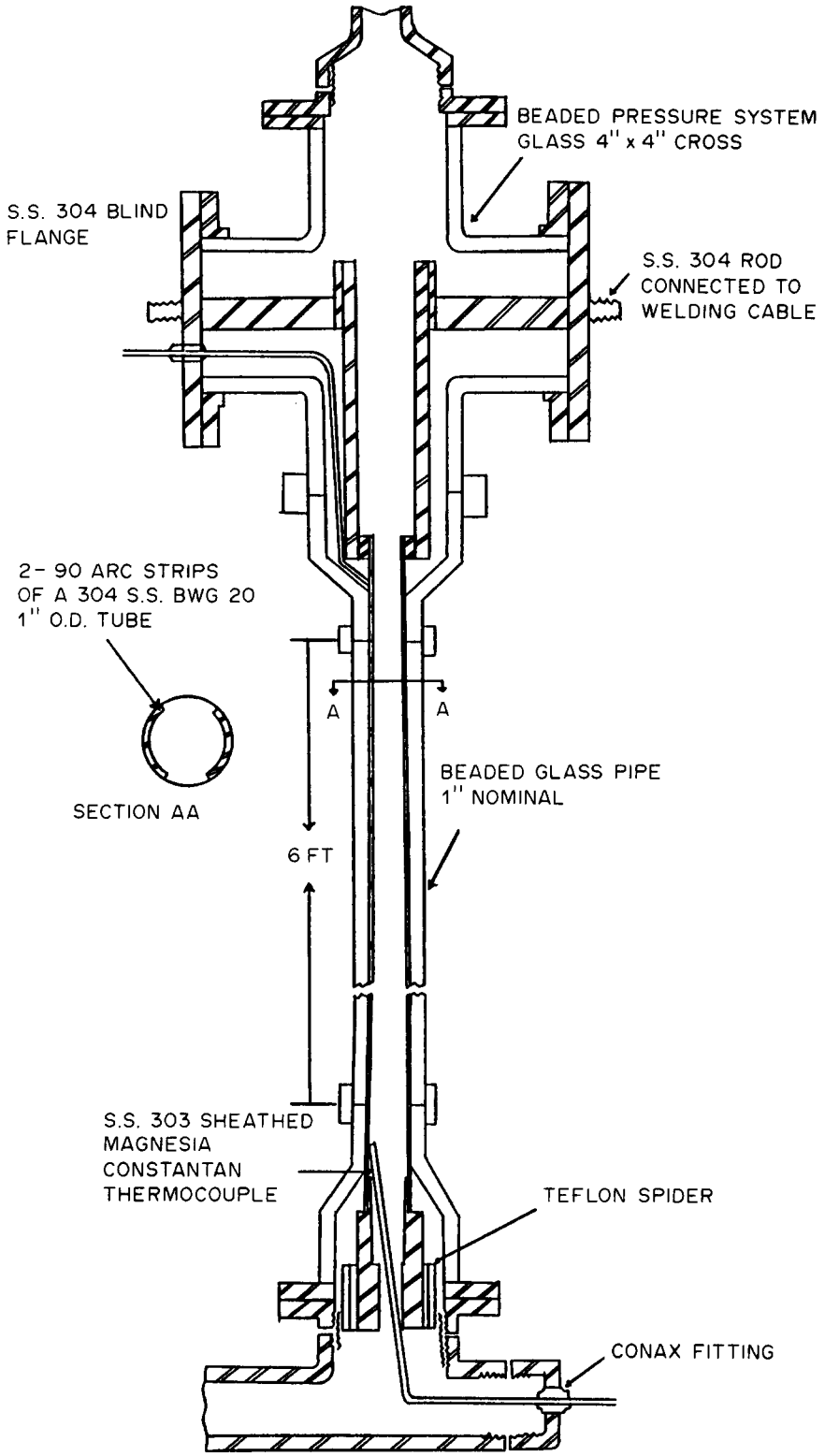

Figure 3. Cross-sectional view of the test section.

To provide a basis for comparison under identical geometrical conditions, flow pattern maps were also determined under adiabatic conditions (heaters off) using the test section shown in figure 3. In the adiabatic case, the external loop heaters provided the heat required. Adiabatic flow pattern observations were taken near the upper end of the test section.

3. RELATIONSHIP BETWEEN INTERFACIAL SHEAR AND FLOW PATTERN TRANSITIONS

3.1. Adiabatic upflow

Superimposed on the $C_D A_{FG}$ curves of figures 1 and 2 are lines showing the transitions between the bubbly, intermittent and annular flow patterns. Examination of these figures suggests that there is a relationship between the values of $C_D A_{FG}$ and the observed flow pattern transitions. The transition between bubbly and intermittent flow seems to occur very near the peak value of $C_D A_{FG}$. Annular flow, on the other hand, is confined to a region of very low values for $C_D A_{FG}$ which corresponds closely to the values predicted by Ying & Weisman (1988) for annular flow. These observations, together with the previous assumption that fully dispersed flow corresponds to zero interfacial shear, led to the following postulates for upward flow:

1. The transition from bubbly to intermittent flow occurs at the peak values of $C_D A_{FG}$.
2. The transition to annular flow occurs at the intersection of the observed values of $C_D A_{FG}$ and the $C_D A_{FG}$ prediction for the annular region (which corresponds to the intersection of interfacial shear predictions for the intermittent and annular regions).
3. The onset of dispersed flow occurs where the value of $C_D A_{FG}$ approaches zero.

Predictions of the flow pattern transitions based on the foregoing criteria are compared with the adiabatic experimental observations of the present study in figure 6. These experimental observations are close to those previously presented by Weisman & Kang (1981).† The current experimental observations of the dispersed flow transition have been augmented at high void fractions by following the transition line extension recommended by Crawford *et al.* (1985). The high void extension of Crawford *et al.* (1985) is based on a correlation of data in the literature and is consistent with present observations at lower void fractions. The recommendation of Crawford *et al.* is supported by the work of Weisman *et al.* (1988). These latter investigators noted that this transition, including its bend to the left at high voids, may be reasonably approximated by

$$\left[\frac{\left(\frac{dp}{dz}\right)g_c}{(\rho_L-\rho_G)g}\right]^{1/2}\left[\frac{\sigma g_c}{(\rho_L-\rho_G)D^2 g}\right]^{-1/4}=1.7. \qquad [4]$$

Earlier expressions for this transition line which used the pressure gradient for liquid flowing alone, $(dp/dz)_{SD}$, in place of the total (dp/dz), did not correctly model the behavior at very high gas flow rates.

The predictions shown in figure 4 for the transitions to bubbly and dispersed flow are based directly on the values of $C_D A_{FG}$ shown in figure 1, which were computed from the observed void fraction vs quality. It may be seen that the transition to bubbly flow, based on the position of the peak in the curve of $C_D A_{FG}$ vs ϵ, is in reasonable agreement with the observations. At void fractions <0.8, the prediction and observed transition to dispersed flow must agree since the $C_D A_{FG}$ curves were derived by setting $C_D A_{FG}=0$ at a mass flow of 1.5×10^7 kg/m^2 h. However, we also find that extrapolation of the curves at lower mass fluxes curves to a zero value of $C_D A_{FG}$ leads to the dispersed flow boundary bending to the left at high void fractions. It may be seen that the predicted boundary at high void fractions, which is between fog and annular flow, is slightly below that suggested by Crawford *et al.* (1985) but shows the same trend.

The transition between annular and intermittent flow is based on the intersection of the values of $C_D A_{FG}$ from the ϵ vs x curves and annular flow models for interfacial shear derived by Ying & Weisman (1988). It will be seen that reasonable agreement with the observed transition is again obtained.

†The experimentally based flow pattern maps for refrigerant 113 shown in figures 7 and 8 of Weisman & Kang's (1981) paper have a scale error. The ordinate scale of those maps should be multiplied by a factor of 10. The generalized flow maps shown in figures 17 and 18 their paper are correct.

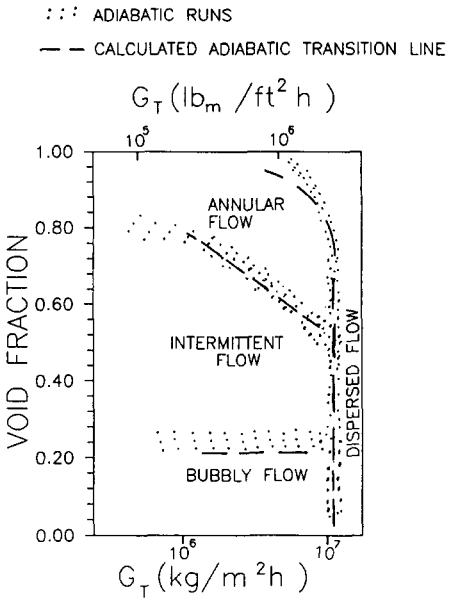

Figure 4. Comparison of predicted and observed flow pattern transitions in adiabatic upflow (refrigerant 113 at 2 b).

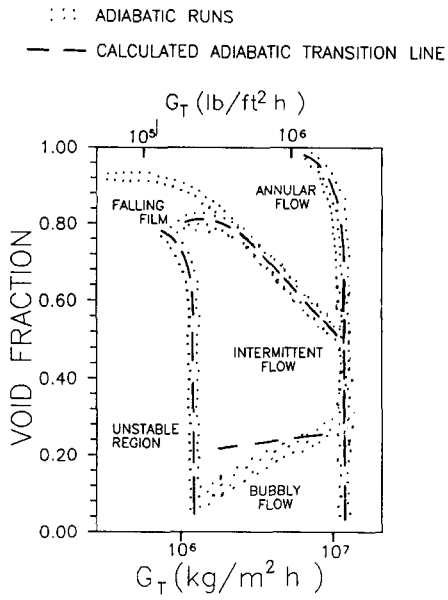

Figure 5. Comparison of predicted and observed flow pattern transitions in adiabatic downflow (refrigerant 113 at 2 b).

The applicability of the proposed relationships between interfacial shear and flow pattern transition to other systems was examined using the steam–water system at 18 b. Ying & Weisman (1988) computed values of $C_D A_{FG}$ as a function of G and ϵ using Marcheterre & Petrick's (1960) relative velocity (slip) correlation for high-pressure steam–water. Application of the proposed transition criteria was based on interfacial shear yield transition lines, which are in fairly good agreement with the predictions of the Weisman & Kang (1981) flow map, as modified by Crawford *et al.* (1985). The dispersed flow transition line, computed from extrapolation of the $C_D A_{FG}$ curves to zero shear, again shows that the transition moves to lower mass velocities as the void fraction increases. These lines show a somewhat more rapid decrease in G than indicated by Crawford *et al.* (1985). However, they are in fairly good agreement with the predictions of Lorenzini & Crescentini (1986) for the fog flow–annular boundary in steam–water systems.

It should be noted that the proposed flow pattern transition criteria are implicitly contained within the Ying & Weisman (1988) interfacial shear models. At the critical bubble spacing at which bubble agglomeration starts (beginning of intermittent flow), the $C_D A_{FG}$ values reach a maximum due to the reduced area of the larger bubbles at higher void fractions. The basis for the annular–intermittent transition, the intersection of the annular and intermittent $C_D A_{FG}$ computations, is essentially the same as indicated by the proposed criteria except that computed $C_D A_{FG}$ values replace observed values in the intermittent region. Dispersed flow is assigned zero interfacial shear, which is also in accord with the proposed criteria.

3.2. Flow pattern transitions in adiabatic downflow

Examination of the interfacial shear curves of figure 2 indicates that the same interfacial shear criteria used for upflow may be used to predict the dispersed and bubble–intermittent flow pattern transitions in downflow. However, a revision of the annular transition criterion is needed as the predicted values for $C_D A_{FG}$ in the vicinity of the annular region tend to be slightly below the observed curves. The annular–intermittent transition is therefore taken as the intersection of the $C_D A_{FG}$ predictions for the intermittent and annular regions. As the model of Ying & Weisman (1988) considers falling film flow without entrainment, the shear criteria do not distinguish between falling film and annular flow.

An additional flow pattern region must be considered in downflow. Crawford *et al.* (1985) noted the presence of an unstable region in which the apparatus could not be operated because of very

large fluid velocity fluctuations. However, they did not consider this a flow pattern region with a definite boundary. The present authors' observations strongly suggest that this stability boundary is not governed by piping system characteristics but by flow conditions. Observations of the system indicated that it became unstable when the downward liquid velocity was so low that it was no longer possible to carry the gas bubbles or packets in a downward direction. Cocurrent downward flow is obviously impossible when the gas bubbles and packets move upward. It is therefore postulated that "the unstable region begins when the value of $C_D A_{FG}$ is such as to produce a zero value for the mean gas velocity, V_G."

The predictions of flow pattern transitions based on the experimentally derived interfacial shear are compared in figure 8 with the present experimental flow pattern observations for refrigerant 113 at 2 b in a 2.5 cm tube. The unstable region boundary is based on present observations as well as the original observations of Crawford (1983). The observed dispersed flow transition is again extended to high void fractions following Crawford *et al.*'s (1985) modification. The experimentally derived transitions are shown as shaded bands and the predictions as solid curves. It may be seen that there is generally good agreement between the predicted and observed flow pattern transitions. As noted earlier, the predictions based on interfacial shear are unable to distinguish between falling film and annular flow.

4. BEHAVIOR DURING DIABATIC CONDITIONS

4.1. Effect of heating on void fraction and interfacial shear

As previously indicated, the variation of the void fraction, ϵ, along the heated test section was observed experimentally during the diabatic tests. The observed ϵ vs distance curves were then compared with calculated curves based on the value of quality, x, obtained from the heat input and the previously obtained relationship between ϵ and x under adiabatic conditions. In these computations, due allowance was made for heat losses from the test section and the lack of thermodynamic equilibrium at the lower qualities. In all upflow cases, the diabatic runs showed slightly higher values of ϵ than were predicted (see figure 6 for typical cases). In all downflow cases, the diabatic runs showed lower ϵ values than were predicted (see figure 7 for typical cases). While

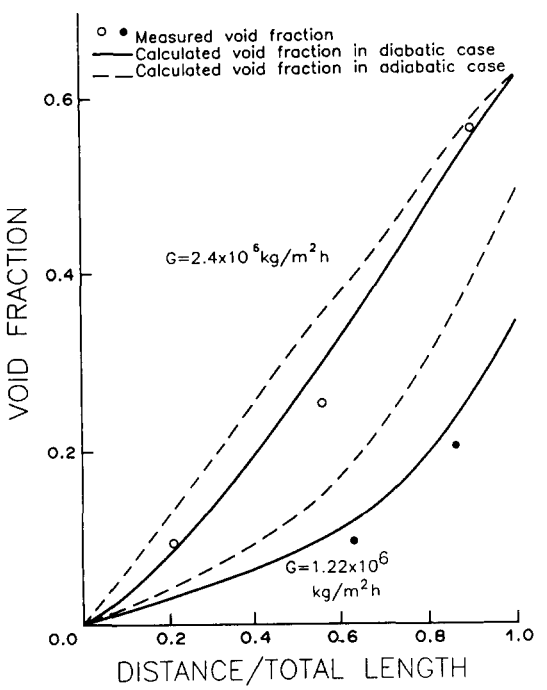

Figure 6. Void fraction vs distance in heated test section for upflow of refrigerant 113 at 2 b (heat flux = 3.8–4.4 × 10^4 W/cm^2).

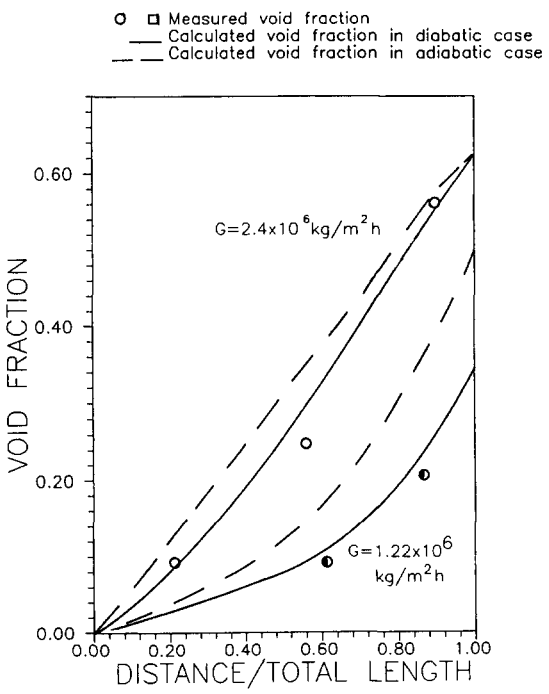

Figure 7. Void fraction vs distance in heated test section for downflow at 2 b, (heat flux = 3.8–5.0 × 10^4 W/cm^2).

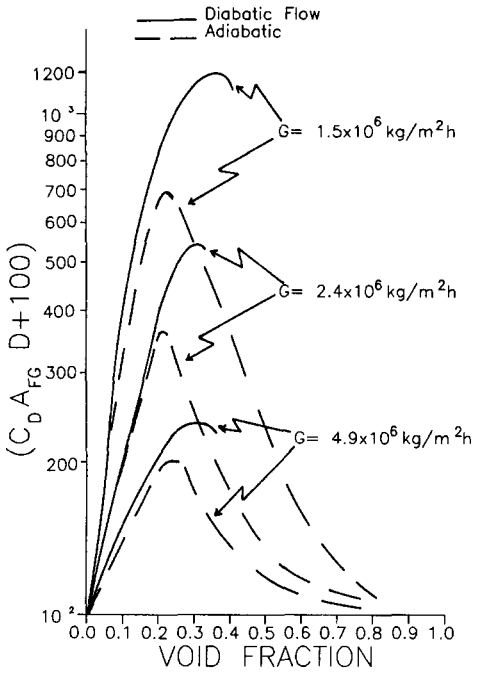

Figure 8. $C_D A_{FG}$ for diabatic upflow of refrigerant 113 at 2 b (heat flux = 3–6 × 10^4 W/cm^2).

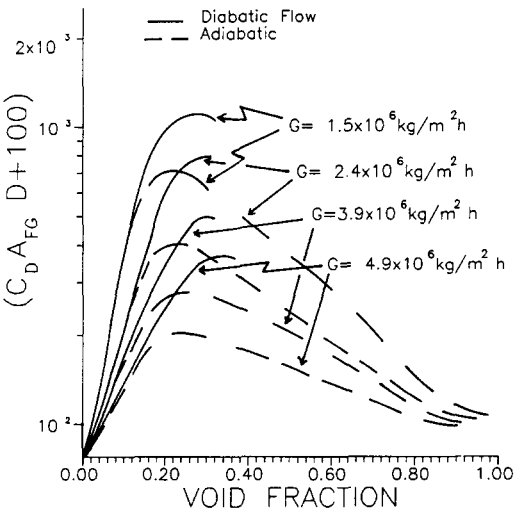

Figure 9. $C_D A_{FG}$ for diabatic downflow of refrigerant 113 at 2 b (heat flux = 3–6 × 10^4 W/cm^2).

errors in estimating the non-equilibrium effect could account for either an upward or downward shift in ϵ, the shift would have the same sign for both upflow and downflow. It was therefore concluded that the observations were truly indicating changes in the ϵ vs x curves.

Curves of ϵ vs x were determined for values of $\epsilon \lesssim 0.5$. The curves could not be determined directly at higher void fractions since reaching high ϵ values required that the inlet fluid contain voids. Conditions then might not fully reflect those of a diabatic test section. Further, the apparatus used provided no way to measure inlet qualities to the test section.

The ϵ vs x curves derived from the diabatic data were therefore used, together with [1], to determine values of $C_D A_{FG}$. The values obtained for upflow and downflow are shown as the solid curves in figures 8 and 9. The tests were carried out in the test section shown in figure 3 at a pressure of 2 b and heater element heat fluxes of between 3 and 6 W/cm^2. It may be seen that the $C_D A_{FG}$ values for diabatic conditions are considerably above those determined for adiabatic flow (dashed curves). In addition, the peak value of $C_D A_{FG}$ occurs at a higher void fraction.

In calculating $C_D A_{FG}$ for the diabatic case, it was assumed that only liquid was in contact with the conduit and heater walls. This assumption is obviously incorrect but it introduces very little error. At $\epsilon < 0.5$, the frictional terms are small with respect to the elevation head. The pressure drop term in [1] is thus considerably larger than the frictional terms and the result is not significantly affected by assumptions relating to the calculation of frictional terms. Values of $C_D A_{FG}$ interpolated from the curves of figures 8 and 9 were used to compute void fraction vs distance for the runs illustrated in figures 6 and 7. As expected, it was observed that the values so computed (see solid curves) provide a good fit of the data.

Estimates of quality were made for a number of cases where $\epsilon > 0.5$ by estimating the entering quality from the entering void fraction and adding the increase in quality due to the heat addition. It appeared that the difference between the adiabatic and diabatic void fraction vs distance curves decreased with increasing quality. In the annular flow region, the difference essentially disappears. An approximate estimate of the $C_D A_{FG}$ curves at $\epsilon > 0.5$ might therefore be obtained by connecting the end of the computed curve with the $C_D A_{FG}$ value on the adiabatic curve at the beginning of annular flow.

4.2. Flow pattern transitions under diabatic conditions

In figures 10 and 11, the flow pattern transitions observed for refrigerant 113 in upflow and downflow under a pressure of 2 b are shown. Both diabatic and adiabatic transitions were observed

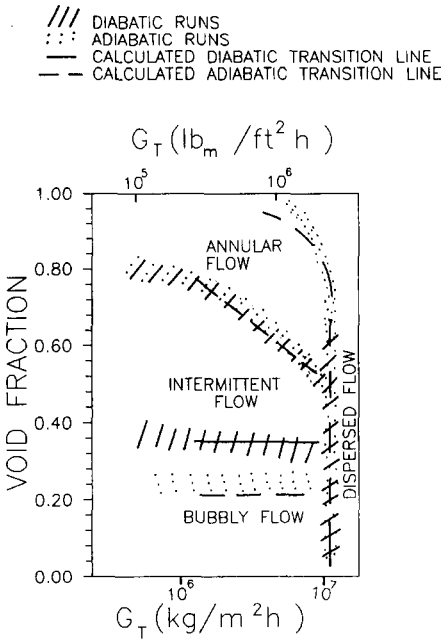

Figure 10. Comparison of flow pattern transitions for diabatic and adiabatic upflow of refrigerant 113 at 2 b (heater strip flux = 3–6 W/cm^2 in the diabatic case).

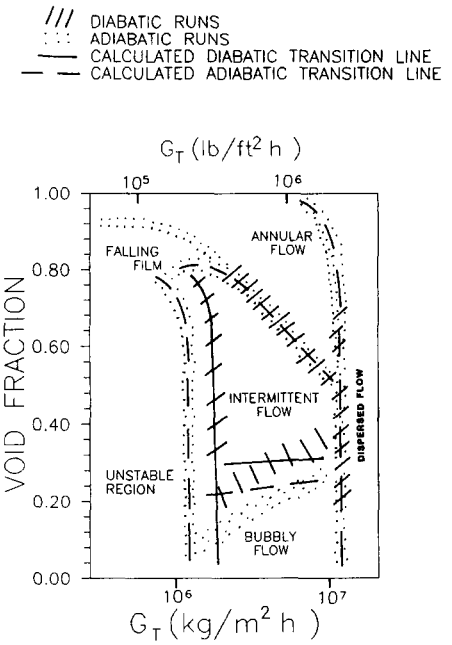

Figure 11. Comparison of flow pattern transitions for diabatic and adiabatic downflow of refrigerant 113 at 2 b (heater strip flux = 3–6 W/cm^2 in the diabatic case).

in the test section illustrated in figure 3. In the diabatic case, heat fluxes on the surface of the heating elements were again in the range of 3–6 W/cm^2.

The flow pattern transitions observed under diabatic conditions are shown by the shaded region and those seen under adiabatic conditions by the dotted regions. The dispersed flow transition observed under adiabatic conditions was again augmented by the dispersed transition region found by Crawford *et al.* (1985) at high void fractions.

It may be seen in figure 10 that the only significant change for upflow is in the bubbly–intermittent transition. This now occurs at higher voids. When we use the previous criterion that the transition occurs at the peak of the $C_D A_{FG}$ curve at any given G, the prediction (solid line) is obtained. It will be observed that the prediction is in good agreement with observations.

The curves of $C_D A_{FG}$ for the diabatic upflow approach those for the adiabatic case as the mass flux is increased. One would therefore expect that the $C_D A_{FG}$ would have a zero value at the same mass flux for both diabatic and adiabatic conditions. The transition to dispersed flow would then remain unchanged. Similarly, the previous suggestion that values of $C_D A_{FG}$ are the same for adiabatic and diabatic conditions when annular flow begins would explain the observation that the transition to annular flow is unchanged.

Examination of figure 11, shows that the behavior of the flow pattern transitions in diabatic downflow is similar to that observed for upflow. The transitions to annular and dispersed flow are again unchanged and the transition from bubbly to intermittent flow occurs at higher void fractions than under adiabatic conditions. In addition, it may be observed that the unstable flow region has expanded.

It will be recalled that in diabatic flow, the peak value of $C_D A_{FG}$ was at a higher void fraction then in adiabatic flow. Prediction of the intermittent–bubbly transition (solid line) based on the position of the peaks in the $C_D A_{FG}$ curves is in reasonable agreement with observations. Predictions of the expanded unstable region boundary also agree with observations. This is explained by the increased values of $C_D A_{FG}$ in diabatic flow which correpond to greater differences between the vapor and liquid velocities. That is, at a given total mass flux, the downward velocity of the vapor will be lower in the diabatic case then in the adiabatic case. Hence, a zero downward velocity (the transition criteria) is found at a higher mass flux. It should be noted that, in obtaining the prediction of the unstable region boundary at high void fractions, the $C_D A_{FG}$ curves were extrapolated to coincide with the adiabatic curves at the onset of annular flow.

4.3. A postulated phenomenologically based explanation of diabatic behavior

Boiling at the heated surface produces numerous small bubbles which are released into the flowing stream. Estimates of the size of the bubbles released using the model of Levy (1966) indicate that the diameter of the bubbles released by the heating surface are in the range of 0.2–0.3 of the equilibrium bubble size used as a base for the estimation of interfacial drag for adiabatic bubbly flow. These small bubbles may be expected to coalesce and gradually be transformed into the larger bubbles typical of adiabatic flow where coalescence and breakup rates are equal. However, the heating surface continuously replenishes the supply of small bubbles. These small bubbles provide a greater interfacial area per unit volume and hence produce the observed augmentation of $C_D A_{FG}$ in the bubbly region.

Bilicki & Kestin (1987) suggested that the bubble–intermittent transition occurs when conditions are such that two aligned bubbles are driven to coalesce by the velocity field in the wake of the forward bubble. This is then translated into a criteria for separation between bubbles. If it is assumed that only the larger equilibrium size bubbles control the transition, the bubble spacing required for transition at diabatic conditions would occur at a higher void fraction than in adiabatic flow. The cloud of smaller size bubbles would add to the void fraction without greatly affecting the spacing between the larger equilibrium bubbles. This would be in accord with the observation that this transition occurs at higher void fractions.

It seems reasonable to suppose that in the intermittent region the absorption of the smaller size bubbles released from the wall into the large vapor regions is more rapid than in bubbly flow. Fewer small bubbles would be present and their effect on interfacial shear would be reduced. This agrees with the observed reduction in $C_D A_{FG}$.

As annular flow is approached, substantial boiling suppression is to be expected. If most of the vapor production is by forced convection vaporization, there would be little surface boiling and few small bubbles.

5. CONCLUSIONS

The relationship between flow patterns and interfacial shear provides an alternative means of determining when flow pattern transitions occur. The shear-based criteria developed here can be useful in some circumstances. In particular, their use in conjunction with appropriate models for interfacial shear can avoid the discontinuities in computed values of $C_D A_{FG}$ which can be imparted by flow pattern transition correlations based on other approaches.

The present study has also pointed out the necessity of considering the unstable region in downflow as the equivalent of a flow pattern. The onset of the unstable region occurs when the value of $C_D A_{FG}$ is such as to produce a zero value for the mean gas velocity.

The shifts in the bubbly–intermittent and unstable region flow transitions, found during the diabatic studies, are consistent with the changes seen in the ϵ vs x relationship and computed values of $C_D A_{FG}$. The shear-based flow pattern transition criteria developed for adiabatic flow are also found to apply under diabatic conditions. Development of a phenomenologically based model of interfacial shear under diabatic conditions would enhance the utility of this approach.

Acknowledgements—The authors wish to acknowledge the financial support of the National Science Foundation which made this work possible. The authors also wish to acknowledge the assistance provided by L. C. Du in completing the calculations for the diabatic studies.

REFERENCES

BILICKI, Z. & KESTIN, J. 1987 Transition criteria for two-phase flow patterns in vertical upward flow. *Int. J. Multiphase Flow* **13**, 283–294.

CRAWFORD, T. J. 1983 Analysis of steady state and transient two-phase flows in downwardly inclined lines. Ph.D. Thesis, Drexel Univ., Philadelphia, Pa.

CRAWFORD, T. J., WEINBERGER, C. D. & WEISMAN, J. 1985 Two-phase flow patterns and void fractions in downward flow. *Int. J. Multiphase Flow* **11**, 761–782.

HUGHES, E. D., LCYZKOWSKI, R. W., MCFADDEN, J. H. & NIEDENAUER, G. F. 1976 An evaluation of state-of-the-art two-velocity two-flow models and their applicability to nuclear reactor transient analysis. Report EPRI-NP-143, Electric Power Research Inst., Palo Alto, Calif.

ISHII, M. & MISHIMA, K. 1980 Study of two-fluid model and interfacial area. U.S. Nuclear Regulatory Commission Report, NUREG/CR-1873 (also ANL-80-111), Argonne National Lab., Argonne, Ill.

LEVY, S. 1966 Forced convection subcooled boiling prediction of vapor volumetric fraction. Report GEAP-515, General Electric Co., San Jose, Calif.

LORENZINI, E. & CRESCENTINI, C. 1986 Determining the two-phase friction coefficient in the transition between annular and fog flow. *Int. J. Heat Mass Transfer* **29,** 507–515.

MARCHETERRE, J. & PETRICK, M. 1960 The prediction of vapor volume fractions in boiling systems. *Nucl. Sci. Engng* **7,** 525.

MCFADDEN, J. H., PAULSEN, M. P. & GOSE, G. C., 1981 RETRAN dynamic slip model. *Nucl. Technol.* **54,** 287.

SOLBRIG, C. W., MCFADDEN, J. H., LCYZKOWSKI, R. W. & HUGHES, E. D. 1975 Heat transfer and friction correlations required to describe steam–water behavior in nuclear safety, studies. Presented at the *15th National Heat Transfer Conf.*, San Francisco, Calif., Paper 21.

WEISMAN, J. & KANG, S. Y. 1981 Flow pattern transitions in vertical and upwardly inclined lines. *Int. J. Multiphase Flow* **7,** 271–291.

WEISMAN, J., BEHBAHANI, A. I. & BHATTACHARYA, S. 1988 An improved representation of the dispersed flow transition. In *Particulate Phenomena and Multiphase Transport* (Edited by VEZIROGLU, T. N.), p. 545. Hemisphere, Washington, D.C.

YING, A. & WEISMAN, J. 1988 Interfacial shear in cocurrent vapor–liquid flow in vertical lines. In *Particulate Phenomena and Multiphase Transport* (Edited by VEZIROGLU, T. N.), p. 555. Hemisphere, Washington, D.C.